Journal of Magnetic Resonance **153,** 138–143 (2001)
doi:10.1006/jmre.2001.2412, available online at http://www.idealibrary.com on IDEAL®

COMMUNICATIONS

Improved Measurement of ^{15}N–{^{1}H} NOEs in the Presence of H(N)-Water Proton Chemical Exchange

Djaudat Idiyatullin, Vladimir A. Daragan, and Kevin H. Mayo[1]

Department of Biochemistry, Molecular Biology, & Biophysics and the Biomedical Engineering Center, University of Minnesota Health Sciences Center, 6-155 Jackson Hall, 321 Church Street, Minneapolis, Minnesota 55455

Received March 21, 2001; revised July 9, 2001; published online October 5, 2001

A simple method is presented to accurately determine ^{15}N–{^{1}H} NOEs in biomolecules in the presence of H(N)-water proton chemical exchange. Three measurements are required: one with nonselective proton saturation and two with different water saturation conditions to determine the equilibrium value of the ^{15}N signal. This approach is exemplified with data on two peptides, one helix-forming 17-mer and one compactly folded 56-mer. Results indicate that ^{15}N–{^{1}H} NOEs determined using the standard approach with short recycle times (3 to 4 s) can be significantly in error when H(N)-water proton chemical exchange is relatively rapid, water proton relaxation is relatively slow, and ^{15}N–{^{1}H} NOEs are away from the value of −1. This new method avoids such inaccuracies resulting from the use of short recycle times.

Key Words: **^{15}N; NOE; NMR; relaxation; chemical exchange.**

INTRODUCTION AND THEORY

Measurement of protein backbone ^{15}N–{^{1}H} NOEs provides important information on the ^{15}N–^{1}H dipolar cross-relaxation term, σ, that is crucial to estimating internal motional correlation times because it is most sensitive to high-frequency spectral densities $J(\omega_N - \omega_H)$ and $J(\omega_N + \omega_H)$. However, the precise measurement of ^{15}N–{^{1}H} NOEs is not trivial due to the influence of chemical exchange between protein backbone amide and water protons (1–3). For any given spin, the NOE enhancement is defined by $(I_{sat} - I_\infty)/I_\infty$, where I_∞ is the equilibrium ^{15}N signal amplitude and I_{sat} is the ^{15}N signal amplitude in the presence of proton saturation. To obtain the correct value for I_∞, very long relaxation delays (recycle times) are usually required to allow for complete relaxation of dynamic processes from both magnetic relaxation and exchange between amide and water protons. Using flip-back pulse sequences (*1*) reduces water saturation, but does not remove this effect completely because of RF field inhomogeneity and radiation damping effects. In protein/water systems, relaxation delays, t, must be greater than 5 times the relaxation time of water protons which could be more than 20 s. Because such delays would make measuring NOEs too time consuming, a standard delay of 3 s is usually used and this often introduces large errors in determining the equilibrium ^{15}N signal amplitude.

The dynamics of ^{15}N and ^{1}H magnetization for amide groups in the presence of water can be described by a set of coupled differential equations (2–4),

$$dN/dt = -R_{1N}(N - N_\infty) - \sigma_{NH}(H - H_\infty) \quad [1a]$$

$$dH/dt = -R_{1H}(H - H_\infty) - \sigma_{NH}(N - N_\infty) - k_1 H + k_2 W - \sigma_{HH}(W - W_\infty) \quad [1b]$$

$$dW/dt = -R_{1W}(W - W_\infty) - \sigma_{HH}(H - H_\infty) + k_1 H - k_2 W, \quad [1c]$$

where N, H, and W are the longitudinal magnetizations for the amide nitrogen, amide proton, and water proton as a function of the recycle time. N_∞, H_∞, and W_∞ are the corresponding equilibrium magnetizations, and R_{1N}, R_{1H}, and R_{1W} are the amide nitrogen, amide proton, and water spin–lattice relaxation rates. σ_{NH} is the cross-relaxation rate between amide nitrogen and proton, σ_{HH} is the cross-relaxation rate between amide and water protons, and k_1 and k_2 are rate constants for amide–water proton chemical exchange. k_1 and k_2 are related by $xk_1 = (1 - x)k_2$, where x is the mole fraction of amide protons. The three equilibrium magnetization terms can be expressed (*2*) as

$$N_\infty \propto x\gamma_N$$
$$H_\infty \propto x\gamma_H \quad [2]$$
$$W_\infty \propto (1 - x)\gamma_H,$$

where γ_H and γ_N are the gyromagnetic ratios of ^{1}H and ^{15}N nuclei, respectively.

[1] To whom correspondence should be addressed. Fax: 612-624-5121. E-mail: mayox001@tc.umn.edu.

1090-7807/01 $35.00

Although the general solution to Eqs. [1] is rather complicated, calculations can be simplified, as is usually the case, by assumming that $R_{1W} \ll R_{1N}$, R_{1H}. When the recycle time is greater than $5/R_{1N}$ and assumming that $dN/dt = dH/dt = 0$, Eqs. [1] can be approximated by

$$N(t) = N_\infty - \frac{\sigma_{NH}(k_2 - \sigma_{HH})(W(t) - W_\infty)}{R_{1N}\left(R_{1H} + k_1 - \sigma_{NH}^2/R_{1N}\right)}, \qquad [3]$$

where t is the recycle time. Due to the relatively high concentration of solvent, water proton dynamics can be dealt with independently from peptide NH protons. This allows the term for water magnetization, $W(t)$, to be expressed as (*4*)

$$W(t) = W_\infty(1 - f) \qquad [4]$$

with

$$f = f(t, b) = \frac{(1 - b)\exp(-Rt)}{1 - b\exp(-Rt)}. \qquad [5]$$

$R = R_{1W} + k_2$, and b is the single-scan saturation factor for water which can be determined experimentally as will be described later. Finally, one has

$$N(t) = N_\infty(1 + af) \qquad [6]$$

with

$$a = \frac{W_\infty\sigma_{NH}(k_2 - \sigma_{HH})}{N_\infty\left(R_{1N} + k_1 - \sigma_{NH}^2/R_{1N}\right)}. \qquad [7]$$

From Eq. [6] it is apparent that the magnetization of ^{15}N nuclei reaches its equilibrium value only after complete relaxation of water magnetization. The constant α describes the influence of proton exchange.

Now let us estimate the systematic error which can be expected if the exchange process is fast, i.e., $k \gg R_{1N}, \sigma_{HH}$. Using expressions [2], Eq. [7] for α becomes

$$a = \frac{\gamma_H\sigma_{NH}}{\gamma_N R_{1N}} = \text{NOE}, \qquad [8]$$

where NOE is the NOE enhancement observed in the absence of exchange. The measured NOE enhancement in the presence of proton exchange (NOE_e) then can be expressed as

$$\text{NOE}_e = \frac{(1 - f)\text{NOE}}{1 + f\ \text{NOE}}. \qquad [9]$$

Figure 1 plots the theoretical curve for NOE_e (solid line) calculated using Eq. [9] with $t = 3$ s, the water spin–lattice relaxation rate $R_{1W} = 0.27\ \text{s}^{-1}$, and the single-scan saturation factor b for water set at 0.5. From Fig. 1, it is apparent that using short recycle times like those commonly employed (3 or 4 s) can lead to

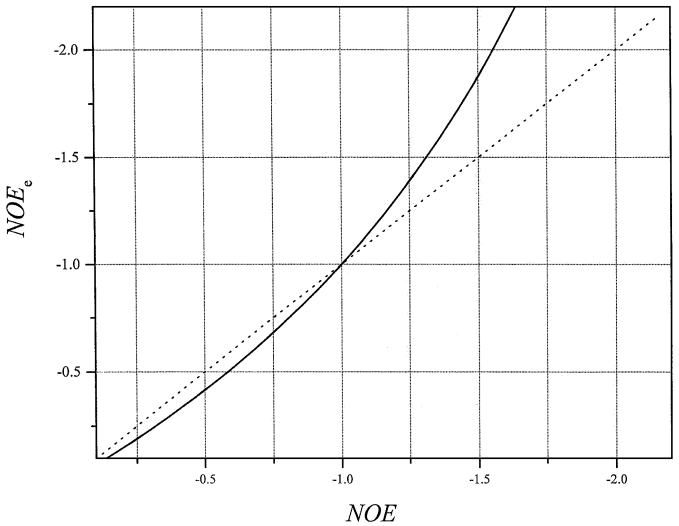

FIG. 1. Theoretical values for the NOE enhancement in the presence of exchange. The theoretical NOE_e curve was calculated using Eq. [9]. This is shown as a solid line. The dashed line is drawn only as a visual aid and represents the situation in the absence of exchange. The NOE_e curve was calculated using $R_{1W} = 0.27\ \text{s}^{-1}$, $t = 3$ s, and $b = 0.5$.

overestimated or underestimated NOE values depending upon whether the NOE is greater than or less than -1, respectively. In particular, large errors can be anticipated for NOE values <-1. Such NOE values are typical for peptides and for protein termini or highly internally mobile segments. Errors can also be significant even when the NOE value is about -0.5. In fact, only when the NOE is close to -1 will errors be minimal.

According to this analysis, experimental results are greatly influenced by the saturation factor b. Later, it will be shown that using the standard water flip-back HSQCSE sequence (*5*), b will be about 0.5 or less. In this case, there are two ways to handle the situation: (1) use a recycle time greater than $5/R_{1W}$, i.e., about 18.5 s in the case above, or (2) use some method to estimate and to compensate for this systematic error. Here, it is proposed that N_∞ be determined by measuring $N(t)$ at two different values of f as defined by Eq. [5]. Using Eq. [6], it can be shown that

$$N_\infty = \frac{N_1 f_2 - N_2 f_1}{f_2 - f_1}, \qquad [10]$$

where N_i and f_i values are measured by using different values of b and/or t [because $f_i = f(t_i, b_i)$] in the HSQCSE pulse sequence. Here, modifications to the HSQCSE pulse sequence are described to achieve this, and this new approach is exemplified with NOE measurements on two peptides.

METHODS AND MATERIALS

The hydrophobic staple α-helix-forming peptide, GFSKAELAKARAAKRGGY (*6*), was synthesized using Fmoc

solid-phase methodology and HPLC purified as described by Idiyatullin *et al.* (*7*). The peptide was isotopically enriched with ^{15}N-amino acids (CIL, Cambridge) at residues F2, A5, L7, A8, and A10. The 56-residue B1 domain from protein G (*8*) was expressed in *Escherichia coli* grown in M9 minimal medium with an ^{15}N–ammonia nitrogen source. The expression vector was generously supplied by Luis Serrano, EMBL, Heidelberg, Germany. Expressed peptide was purified essentially as described by Barchi *et al.* (*8*) with the addition of a final purification step by HPLC using a linear acetonitrile/water gradient. Purity was checked by analytical HPLC and mass spectrometry. Peptide concentration was determined from the dry weight of freeze-dried samples.

For NMR measurements, freeze-dried peptide was dissolved in H_2O/D_2O (90/10). Relaxation experiments were performed on a Varian Inova-500 NMR spectrometer equipped with a triple-resonance probe. For the measurement of ^{15}N–{^{1}H} NOEs, the pulse sequence based on the water flip-back scheme of Farrow *et al.* (*5*) was used as illustrated in Fig. 2A. This pulse sequence was taken from the "ProteinPack" library of pulse sequences provided by Varian Instruments, Inc., and will be referred to as pulse sequence A. The water saturation factor, *b*, can be varied by changing values of the gradient g_1. When $g_1 = 0$ in this flip-back pulse sequence, water saturation will be minimal and *b*, theoretically, will approach unity. On the other hand, when g_1 is not zero, water will be saturated to some extent (equivalent to presaturation of water proton magnetization) and, consequently, *b* will tend toward zero. Using pulse sequence A to determine N_∞ as precisely as possible requires, however, that *b* be varied substantially (*5*), and this cannot always be achieved experimentally.

Here, a novel way to substantially vary *b* is proposed by applying a 180° pulse at the beginning of the RT period in pulse sequence A. Doing this effectively changes the sign of *b* to $-b$. Inversion of proton magnetization is achieved by applying a composite 180° pulse (90*x*–180*y*–90*x*) (*9*) as illustrated in Fig. 2B (scheme Ba). To suppress radiation damping, a series of *n* very weak and uniformly spaced rectangular gradient pulses (*10*), g_9, is employed, and to avoid shifts in the lock that result from use of this long series of gradient pulses, the sign of gradients is changed every 100 ms. For the NOE experiment, nonselective proton irradiation is achieved by applying $\theta = 120°$ pulses spaced at τ_s = 5-ms intervals during RT (*11*) (Fig. 2B, scheme Bb).

The pulse sequence shown in Fig. 2C (pulse sequence C) is used to measure the T_1 of water. Using strong gradient pulses, the amplitude of the Hahn echo is reduced due to diffusion effects, thereby minimizing radiation damping during the detection period. This saturation-recovery method is relatively fast because the recycle time can be set to 0. Values for R_{1W} were obtained by fitting the relaxation curve as $A(t) = A(0)(1 - \exp(\tau_R R_{1W}))$.

To estimate the saturation factor *b* for water, the boxed-in part of pulse sequence C (scheme Ca) replaces the detection period

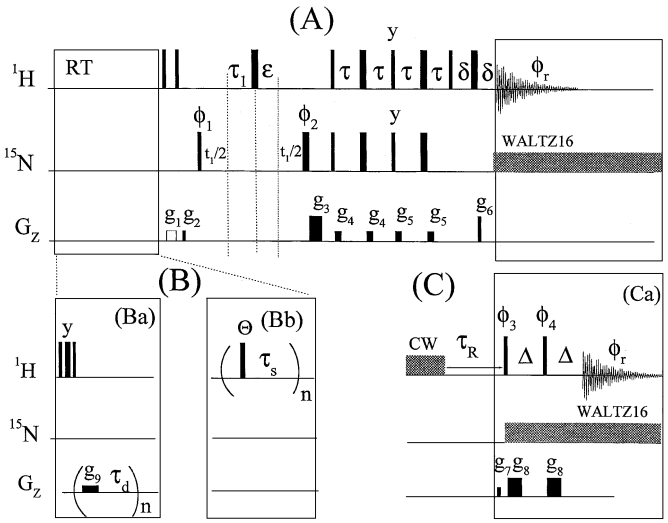

FIG. 2. Modifications to the water flip-back HSQCSE pulse sequence. The pulse sequence commonly used for measuring ^{15}N–{^{1}H} NOEs, which is based on the water flip-back pulse sequence of Farrow *et al.* (*5*), is shown in (A). This pulse sequence is referred to as pulse sequence A in the text. The pulse sequences shown in schemes Ba and Bb are used in combination with pulse sequence A (RT period) to invert proton magnetization, thereby changing the sign of the saturation factor *b* (Ba), and to saturate proton resonances (Bb). The pulse sequence shown in scheme C (pulse sequence C) is used to measure T_1 values of water. The boxed-in part of this pulse sequence (scheme Ca) is used in combination with pulse sequence A (detection period) to measure the *Z*-component of magnetization. Ninety and 180° pulses are represented proportionally by the thickness of the bars. Unless otherwise indicated, all pulses are applied along the *x*-axis. Inversion of proton magnetization (scheme Ba) was achieved by using a composite 180° pulse (90*x*–180*y*–90*x*) (*9*). To suppress radiation damping, a series of *n* very weak and uniformly spaced rectangular gradient pulses (*10*), g_9, is employed, and to avoid shifts in the lock that result from use of this long series of gradient pulses, the sign of gradients is changed every 100 ms. For the NOE experiment, nonselective proton irradiation (scheme Bb) is achieved by applying $\theta = 120°$ pulses spaced at τ_s = 5-ms intervals during RT (*11*). For helix-forming peptide and B1 peptide experiments, RT was 4 and 3 s, respectively, and was the same for NOE and no-NOE measurements with different water saturation factors. τ_R is the recovery time. Delays were set as follows: $\delta = 0.48$ ms, $\tau = 2.22$ ms, $\tau_1 = 2.57$ ms, $\varepsilon = 1.2$ ms, and $\Delta = 20$ ms. Gradient values were: $g_1 = 4.28$ G cm^{-1} for 1 ms (in the water flip-back scheme, $g_1 =$ 0, 0 G cm^{-1}); $g_2 = 3$ G cm^{-1} for 1 ms; $g_3 = 42.9$ G cm^{-1} for 3.73 ms; $g_4 =$ 1.85 G cm^{-1} for 0.2 ms; $g_5 = 2.78$ G cm^{-1} for 0.2 ms; $g_6 = 41.17$ G cm^{-1} for 0.373 ms; $g_7 = 9$ G cm^{-1} for 2.4 ms, and $g_8 = 53.26$ G cm^{-1} for 3 ms. Phase cycling for pulse sequence A was $\phi_1 = y, -y$; $\phi_2 = x, x, y, y, -x, -x, -y, -y$, and $\phi_r = x, -x, -x, x$. Phase cycling for the pulse sequence shown in scheme C was $\phi_3 = -x, x$; $x, -x$; $\phi_4 = y, y, -y, -y$, and $\phi_r = x, -x, -x, x$. CW (continuous wave) decoupling was used with a 1-kHz field for 2 s, RT = 0. For ^{15}N decoupling, WALTZ-16 was achieved by using a 1.8-kHz RF field.

(also boxed-in) in pulse sequence A. In order to measure the saturation factor *b* for water with pulse sequence A (Fig. 2), the amplitude of equilibrium magnetization and the *Z*-component at the beginning of the detection period had to be measured. Figures 3a and 3b exemplify this by showing spectra for the B1 peptide obtained using (a) only the pulse sequence shown in scheme Ca and (b) pulse sequence A without proton saturation

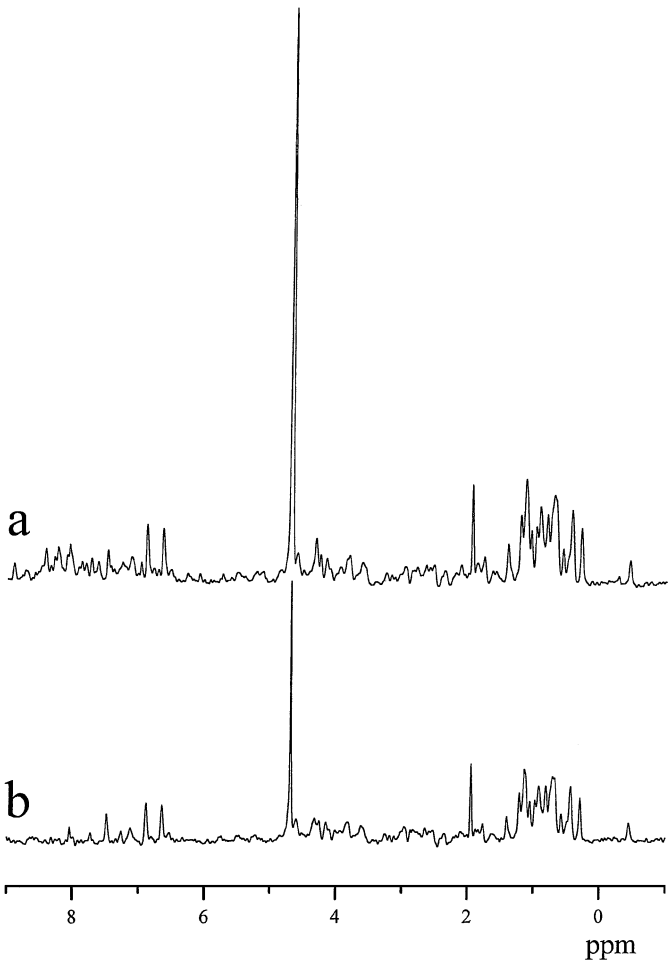

FIG. 3. ^{1}H NMR spectra of the B1 peptide. Two ^{1}H NMR spectra of B1 peptide are shown. These spectra were obtained by using the pulse sequence Ba (Fig. 2) without (a) and following (b) the flip-back scheme of pulse sequence A (Fig. 2A). In both cases, proton saturation was not used during the RT period which was equal to 20 s.

during RT but with incorporation of scheme Ca as described above. In both cases, RT was 20 s. Because the diffusion coefficient of water is much larger than that of the peptide, the water signal at 4.75 ppm was dramatically reduced, becoming comparable to resonances arising from the B1 peptide. For peptide proton resonances, the saturation factor is about 0.8, which can be explained by the presence of RF field inhomogeneity. In spectrum 3b, amide proton resonance amplitudes are attenuated. This is due to the fact that at the beginning of the detection period in pulse sequence A, amide proton magnetization lies in the *XY* plane and is not detectable using scheme Ca, which is designed to detect magnetization oriented along the *Z*-axis. For water, the saturation factor is about 0.5, which is quite different from saturation factors of proton resonances from the peptide. This difference arises from radiation damping that occurs using pulse sequence A, and this prevents effecient successive water flip-backs.

RESULTS AND DISCUSSION

To exemplify this approach, results are presented on two ^{15}N-enriched peptides: an α-helix-forming 17-mer GFSKA$_5$EL$_7$AKARAAKRGGY (6) and the compactly folded 56-residue B1 domain from protein G (*8*). To illustrate how partially saturated water affects ^{15}N equilibrium magnetization during an NOE experiment, Fig. 4 plots the backbone ^{15}N signal amplitude of residues A5 and L7 from the α-helix-forming peptide as a function of the pulse sequence repetition time. At short recycle times, intensities are negative due to the negative value of the ^{15}N–{^{1}H} NOE and the effect of H(^{15}N)-water proton exchange. Signal amplitudes then grow monotonically and plateau off at their equilibrium value by about 20 s, i.e., after complete relaxation of the water proton signal. Therefore, in order to get accurate ^{15}N–{^{1}H} NOEs using the normally employed approach, a recycle time of at least 20 s should actually be used. The recycle time, of course, depends on sample conditions, e.g., temperature and viscosity, and on the particular NH, i.e., the lifetime of the proton in the biomolecule and the exchange rate of that proton with protons from water.

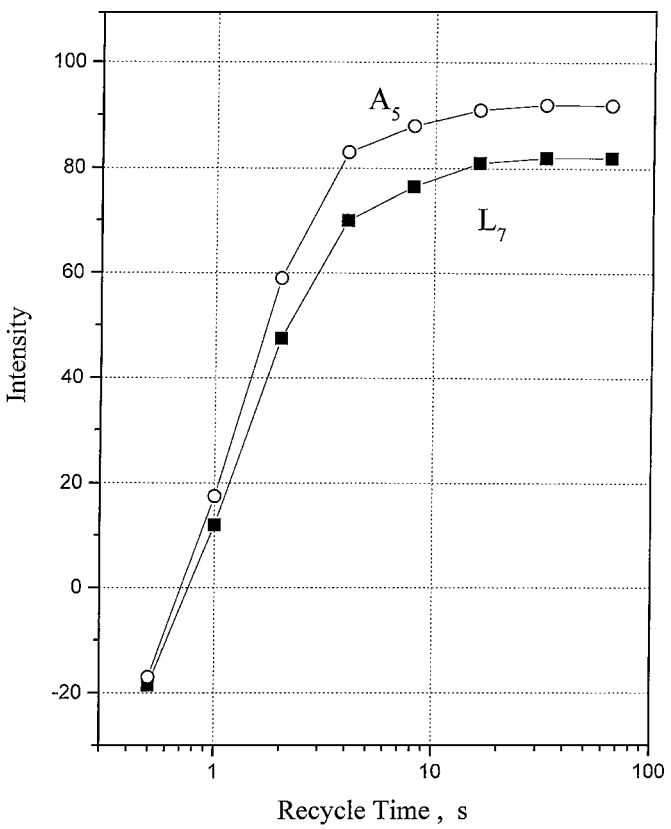

FIG. 4. Dependence of ^{15}NH magnetization on the recycle time. ^{15}NH signal intensity is plotted vs the recycle time in an ^{15}N–{^{1}H} NOE experiment using pulse sequence A (Fig. 2A) without proton saturation. Data acquired at 30°C are shown for two residues, A5 (open circles) and L7 (filled squares), from the helix-forming peptide as discussed in the text. Lines connecting data points are drawn as visual aids.

The use of one, relatively short recycle time (3 or 4 s commonly employed) is usually not sufficient to accurately measure all ^{15}N–{^{1}H} NOEs in a given biomolecule. To demonstrate this point, Fig. 4 compares ^{15}N–{^{1}H} NOEs measured with the α-helix-forming peptide using the standard NOE approach (open symbols) and this new approach (filled symbols). Both sets of experiments were performed using a recycle time of 4 s, and data are shown for two temperatures, 5 (squares) and 30°C (circles). ^{15}N–{^{1}H} NOEs are plotted vs the sequence position of the five residues in the peptide that were ^{15}N-enriched: F2, A5, L7, A8, and A10. The latter four residues are located within the α-helix-forming part of the peptide, whereas F2 is part of the hydrophobic staple region of the peptide. At 5°C, the peptide is highly structured (*6*) and the molecule tumbles more slowly in solution giving rise to more positive ^{15}N–{^{1}H} NOEs, whereas at 30°C, the peptide is mostly unstructured and the molecule tumbles more rapidly in solution giving rise to more negative ^{15}N–{^{1}H} NOEs. This temperature-dependent effect on ^{15}N–{^{1}H} NOEs was expected. However, notice that in either case, measured values for NOEs are different from one experimental approach to the other. Differences are greater for NOE values further away from -1. At NOE values more positive than -1, the standard approach systematically yields more positive NOEs, whereas at NOE values more negative than -1, the standard approach systematically yields more negative NOEs. This is consistent with the behavior of the calculated curve shown in Fig. 1. The difference in calculated NOE values using these approaches is strikingly evident for residue F2 at 30°C. It should be emphasized that, in all cases, ^{15}N–{^{1}H} NOEs determined using the new approach are the same as ^{15}N–{^{1}H} NOEs determined using the standard approach with a longer recycle time of 20 s. In normal instances, such recycle times would not be used due to excessive spectrometer time required for these experiments.

The dramatic difference in ^{15}N–{^{1}H} NOE values determined using these two approaches is not due to poor signal-to-noise in any one of the component NOE spectra. As shown in the inset to Fig. 5, signal-to-noise for F2, A5, L7, and A8 is very good in all three component spectra: (a) without saturation, (b) without saturation, but with changing the sign of the saturation factor, *b*, and (c) with proton saturation. Spectra a and c are used to calculate the value of the NOE using the standard approach, and spectrum b is the additional experiment required to calculate NOEs using this new approach. The equilibrium signal for F2 is the smallest of all residues because H(N)-water proton exchange rate, which is faster for F2 than for the other residues, significantly reduces the ^{15}NH signal amplitude during polarization transfer in the INEPT pulse sequence. However, this does not affect the actual value of the calculated NOE because signal attenuation occurs equally in all component spectra and the NOE is due, in any event, to ^{1}H–^{15}N dipole–dipole interactions. Three reasons account for differences in NOE values calculated using these two approaches: (1) relatively rapid H(^{15}N)-water proton exchange which significantly affects the value of N_∞, (2) the relaxation time of water protons, and (3) the relative magnitude of

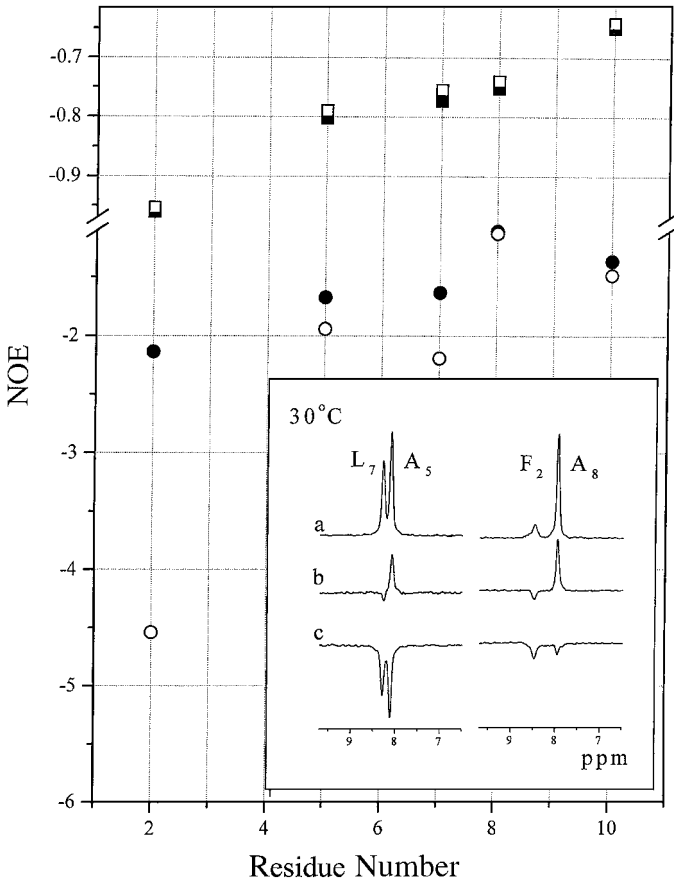

FIG. 5. ^{15}N–{^{1}H} NOEs from the helix-forming peptide. ^{15}N–{^{1}H} NOEs, calculated using the new approach (filled symbols) and the standard approach (open symbols) as discussed in the text, are plotted vs the residue number for the amino acid sequence of the helix-forming peptide. ^{15}N–{^{1}H} NOEs are shown for data acquired at two temperatures, 5 (squares) and 30°C (circles). The insert at the lower right shows component ^{15}NH spectra used to calculate ^{15}N–{^{1}H} NOEs for residues F2, A5, L7, and A8 of the peptide. These data were acquired at 30°C. For each residue shown, the component NOE spectra are (a) without saturation, (b) without saturation, but with a change in the sign of the saturation factor, *b*, and (c) with proton saturation.

the actual NOE. This last point is exemplified by data acquired on the helix-forming peptide at 5°C where all five NOEs are comparatively nearly the same, being different only by about a few percent, because their values are close to -1. The accuracy of ^{15}N–{^{1}H} NOEs determined using the standard approach is very much dependent on these three factors.

With a compactly folded peptide like the B1 domain from protein G, the situation is not much better. As with the helix-forming peptide, ^{15}N–{^{1}H} NOEs were determined using both approaches, but with a recycle time of 3 s. In this example, moreover, ^{15}N–{^{1}H} NOE data were measured on a uniformly ^{15}N-enriched peptide using the 2D NMR version of pulse sequence A with our modifications. NOE data on the helix-forming peptide presented above and shown in Fig. 5 were acquired using the one-dimensional version of this modified pulse sequence.

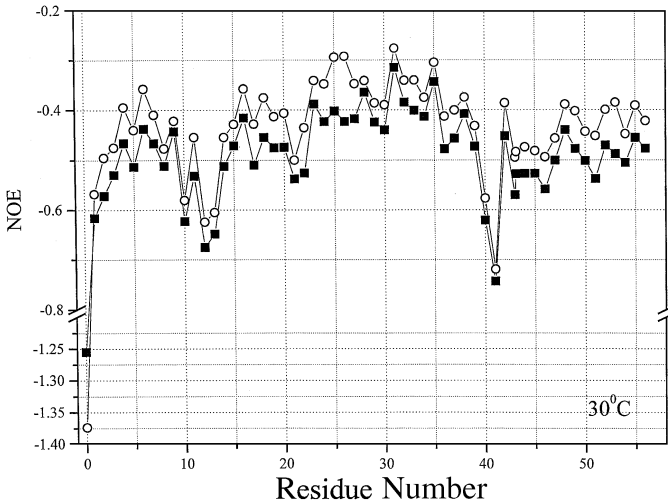

FIG. 6. ^{15}N–{^{1}H} NOEs from peptide B1 from protein G. ^{15}N–{^{1}H} NOEs calculated using the new approach (filled squares) and the standard approach (open circles), as discussed in the text, are plotted vs the residue number for the amino acid sequence of peptide B1 from protein G. ^{15}N–{^{1}H} NOEs are shown for data acquired at 30°C.

Figure 6 plots ^{15}N–{^{1}H} NOEs from the 56-residue B1 peptide as a function of its sequence. Open circles give values for NOEs calculated using the standard approach, and filled squares give NOEs calculated using the new approach. As noted above with the helix-forming peptide, NOEs having values more positive than −1 are systematically calculated to be more positive with the standard approach and those NOEs having values more negative than −1 are systematically calculated to be more negative. This is exemplified by the highly mobile N-terminal residue which exhibits an NOE of about −1.4. Other NOEs through the sequence are more positive than −1. In any event, it is apparent that measuring ^{15}N–{^{1}H} NOEs without taking into account H(^{15}N)-water proton exchange can introduce substantial error. Notice that some NOEs for the B1 peptide are shifted by more than 0.1. Such inaccuracies in NOE values will lead to inaccuracies in motional parameters derived using a motional model. Any significant increase in the value of the NOE will result in larger motional order parameters using, for example, the Lipari–Szabo model free analysis (*12*, *13*), and NH vectors in the peptide would be interpreted as being more motionally restricted than they actually are.

In conclusion, this new experimental approach yields more accurate values for ^{15}N–{^{1}H} NOEs measured in cases where the H(^{15}N)-water proton exchange rate is sufficiently rapid to affect amplitudes of signals in equilibrium ^{15}NH spectra acquired at relatively short recycle times. This is of particular concern for ^{15}N–{^{1}H} NOEs that are away from a value of −1.

ACKNOWLEDGMENTS

This work was supported by research grants from the National Institutes of Health (NIH, GM-58005) and the National Science Foundation (NSF, MCB-9729539) and benefited from use of the high field NMR facility at the University of Minnesota.

REFERENCES

1. S. Grzesiek and A. Bax, The importance of not saturating H_2O in protein NMR. Application to sensitivity enhancement and NOE measurements, *J. Am. Chem. Soc.* **115,** 12593–12594 (1993).
2. N. J. Skelton, A. G. Palmer III, M. Akke, J. Koerdel, M. Rance, and W. J. Chazin, Practical aspects of two-dimensional proton-detected ^{15}N spin relaxation measurements, *J. Magn. Reson. B* **102,** 253–264 (1993).
3. E. Baguet and C. Roby, Off-resonance irradiation effect in steady-state NMR saturation transfer, *J. Magn. Reson.* **128,** 149–160 (1997).
4. R. R. Ernst, G. Bodenhausen, and A. Wokaun, "Principles of Nuclear Magnetic Resonance in One and Two Dimensions," Clarendon Press, Oxford (1987).
5. N. Farrow, R. Muhandiram, A. Singer, S. Pascal, C. Kay, G. Gish, S. Shoelson, T. Pawson, J. Forman-Kay, and L. Kay, Backbone dynamics of a free and phosphopeptide-complexed Src homology 2 domain studied by ^{15}N NMR relaxation, *Biochemistry* **33,** 5984–6003 (1994).
6. V. Munoz, F. J. Blanco, and L. Serrano, The hydrophobic-staple motif and a role for loop-residues in α-helix stability and protein folding, *Struct. Biol.* **2,** 380–385 (1995).
7. D. Idiyatullin, A. Krushelnitsky, I. Nesmelova, F. Blanco, V. A. Daragan, L. Serrano, and K. H. Mayo, Internal motional amplitudes and correlated bond rotations in an α-helical peptide derived from ^{13}C and ^{15}N NMR relaxation, *Protein Sci.* **9,** 2118–2127 (2000).
8. J. J. Barchi, B. Grasberger, A. M. Gronenborn, and G. M. Clore, Investigation of the backbone dynamics of the IgG-binding of streptococcal protein G by heteronuclear 2D ^{1}H–^{15}N NMR, *Protein Sci.* **3,** 15–21.
9. M. N. Levitt and R. Freeman, NMR population inversion using a composite pulse, *J. Magn. Reson.* **33,** 473–476 (1979).
10. W. S. Price, K. Haymizu, and Y. Arata, Optimization of water-PRESS pulse sequence and its integration into pulse sequences for studying biological macromolecules, *J. Magn. Reson.* **126,** 256–265 (1997).
11. J. L. Markley, W. J. Horsley, and M. P. Klein, Spin–lattice relaxation measurement in slowly relaxing complex spectra, *J. Chem. Phys.* **53,** 3604–3605 (1971).
12. G. Lipari and A. Szabo, Model-free approach to the interpretation of nuclear magnetic resonance relaxation in macromolecules. I. Theory and range of validity, *J. Am. Chem. Soc.* **104,** 4546–4559 (1982).
13. G. Lipari and A. Szabo, Model-free approach to the interpretation of nuclear magnetic resonance relaxation in macromolecules. II. Analysis of experimental results, *J. Am. Chem. Soc.* **104,** 4559–4570 (1982).